cytiva

Imaging technologies supporting emerging research

Amersham™ Typhoon™ laser scanner applications and impact

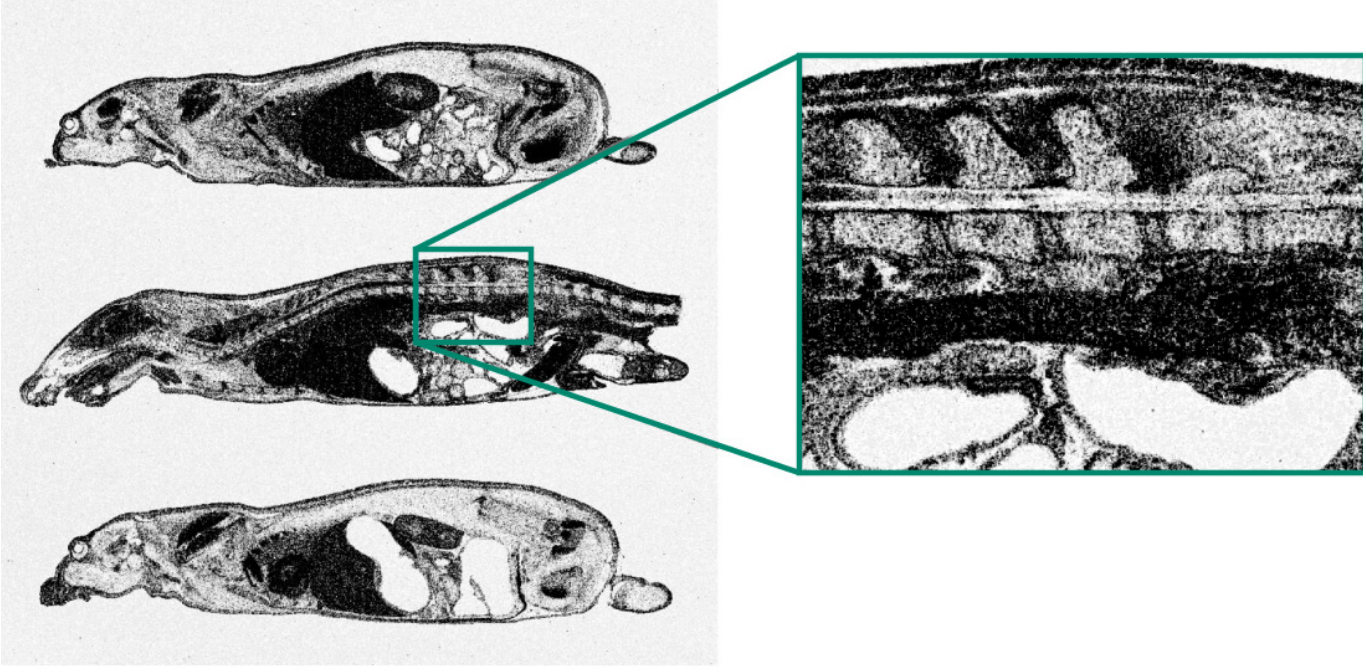

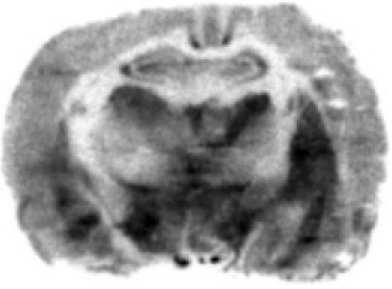

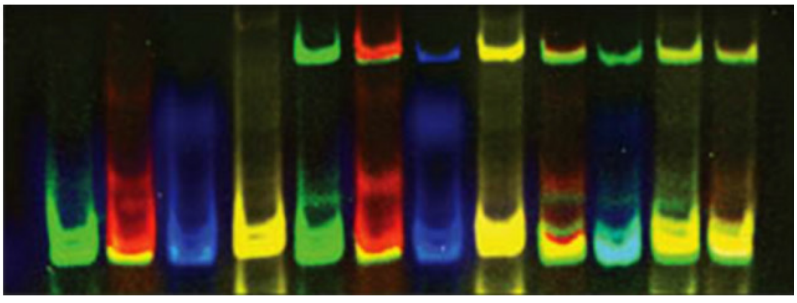

cytiva.com

Contents

Introduction

Biomolecular imaging tools, designed for the precise quantification of proteins, nucleic acids, and other biomolecules, play a critical role in all areas of life sciences. Imaging tools enable researchers to explore cellular mechanisms by offering quantifiable insights into gene expression, protein interactions, and molecular pathways. The evolution of these imaging tools is marked by significant advancements, from basic colorimetric and radiographic detection, to sensitive, high-resolution methods like fluorescence imaging. Now, all of these methodologies are supported by advanced, multifunctional devices, like Amersham™ Typhoon™ biomolecular imagers: sensitive, modular scanners designed for versatile imaging and precise quantification of fluorescent, colorimetric, and radiolabeled proteins and nucleic acids.

Such advancements have enhanced our ability to quantify and visualize biomolecules with exceptional precision, facilitating a deeper understanding of biological processes and disease mechanisms. In this review, we explore key features of the Amersham Typhoon imagers in detail and delve into their applications and impact across life sciences.

We also examine breakthrough biological research supported by the imaging capabilities of the Amersham Typhoon laser scanner.

Applications of the Amersham Typhoon imagers

Due to their highly flexible nature and capacity to support imaging of near-infrared (NIR), fluorescence, radioactive, and colorimetric labeled molecules, Amersham Typhoon scanners are used for various applications across the biomedical sciences. Table 1 summarizes recent Springer- and Scopus-indexed publications that leveraged Amersham Typhoon scanners in their studies, some of which will be explored in detail in the following sections.

Table 1. Estimated days saved by high-seed over conventional seeding

Application	Assay	Research Area	Reference
Immunoblotting	Western blotting/ dot blotting	Cell biology	(1–3)
		Molecular biology	(4)
		Neurobiology	(5–7)
		Oncology	(8–10)
		Parasitology	(11, 12)
		Plant biology	(13)
	Northern blotting	Genetics	(14)
		Genomics	(15, 16)
		Molecular biology	(17–19)
		Neurobiology	(7)
		Plant biology	(20, 21)
		Structural biology	(22)
		Virology	(23)
	Southern blotting	Molecular biology	(24, 25)
		Oncology	(26, 27)
		Plant biology	(28)
	Thin layer chromatography	Clinical tool development	(29–33)
		Microbiology	(34)
		Neurobiology	(35, 36)
		Parasitology	(37)
		Structural biology	(38, 39)
Phosphor imaging		Cell biology	(40–43)
		Clinical tool development	(29–31, 33, 44–48)
		Microbiology	(18, 34)
		Molecular biology	(19, 24, 25, 49–51)
		Neurobiology	(7, 36, 52)
		Oncology	(26, 53, 54)
		Parasitology	(37, 55)
		Plant biology	(15, 56)
		Radiochronometry	(57)
		Structural biology	(58, 59)
		Virology	(23, 60–63)
Electrophoretic mobility shift assay		Immunology	(64–66)
		Microbiology	(67–69)
		Molecular biology	(4, 70–74)
		Oncology	(53)
		Structural biology	(75–77)
Stain dye-based gel plate visualization	Phosphoprotein imaging	Plant biology	(78, 79)
	Protein peptide imaging	Molecular biology	(80–82)
		Structural biology	(83)
	Nucleotide imaging	Cell biology	(84)
		Clinical tool development	(85)
		Immunology	(64)
		Molecular biology	(74, 86)
		Research tool development	(87, 88)
		Structural biology	(89)

Immunoblotting

Western blotting

Perhaps the most widely used immunoblotting technique in molecular biology and biochemistry, Western blotting separates proteins by molecular weight through gel electrophoresis (1). The proteins in the gel are then transferred onto a membrane, which can be imaged using a molecular scanner, such as an Amersham Typhoon imager, producing a band for each protein. Western blotting is a simple and inexpensive method for identifying changes in protein expression or interactions between different samples, and is widely used across various areas of life sciences. Each use case described here applied an Amersham Typhoon scanner to Western blotting membranes, which helped researchers decipher fascinating and clinically relevant research findings.

In their 2023 publication, Drobny and colleagues used a combination of Western blotting and immunocytochemistry to examine the effect of intracellular alpha-synuclein (αSyn) levels on cell homeostasis and lysosomal function in Parkinson's disease (PD) patient-derived dopaminergic neurons (2). Through robust biochemical analysis using an Amersham Typhoon Biomolecular Imager, they elucidated a novel interplay between αSyn, a characteristic feature of PD and other synucleinopathies, and the enzymatic function of lysosomal cathepsins. Aside from deepening our understanding of the molecular mechanisms underpinning PD, this study holds clinical relevance, suggesting that boosting cathepsins' lysosomal transport may reduce αSyn toxicity in synucleinopathies.

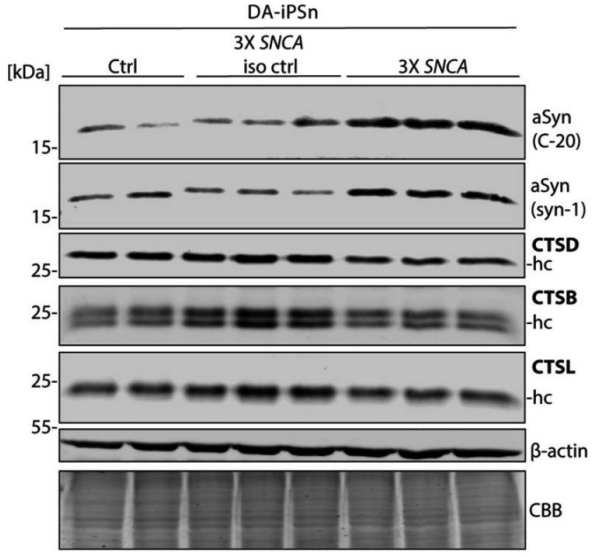

Fig 1. Adapted from Fig 2A (5). Impaired maturation and proteolytic activity of cathepsins in iPSC-derived DA midbrain neurons with pathological αSyn levels. Representative Western blot analysis of Triton-soluble lysates of DA-iPSn of healthy control (ctrl), isogenic control (iso ctrl) and 3 × SNCA showing mature forms (heavy chain; hc) of CTSD, CTSB, and CTSL as well as αSyn. β-Actin served as a loading control.

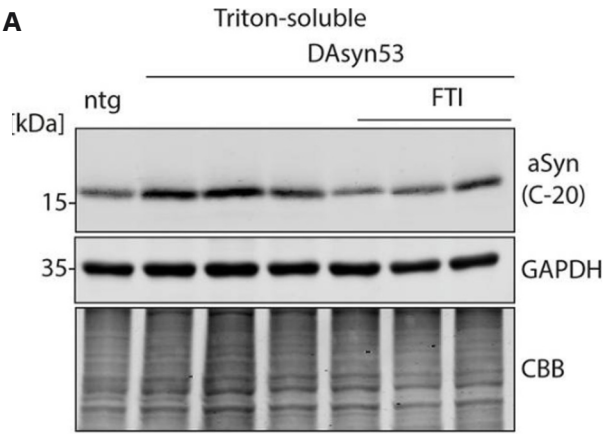

Fig 2. Adapted from Fig 5A (5). Rescue of disrupted cathepsin maturation and activity in mice overexpressing αSyn A53T in dopaminergic neurons. Western blot analysis of αSyn detected with C-20 antibody in thalamus/midbrain Triton-soluble samples of non-transgenic (ntg) mice and mice overexpressing human A53T in dopaminergic neurons (DAsyn53). DAsyn53 mice were treated with FTI for 26 days.

In addition to enabling researchers to pinpoint the molecular basis of disease, Western blotting workflows employing Amersham Typhoon imagers have been applied to develop a novel small cell carcinoma of the ovary hypercalcemic type (SCCOHT) cell line (8). Given the broad use of cell lines as in vitro models across biomedical research (91), the high degree of imaging accuracy facilitated by Amersham Typhoon imagers represents an essential feature in this particular study. The cell line, which was extensively characterized in terms of its morphology, genetic molecules, biological behavior, and tumorigenesis, will likely represent a valuable model for SCCOHT research specific to patients from Asian populations.

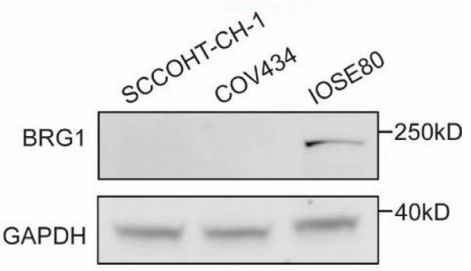

Fig 3. Adapted from Fig 2C (8). Analysis of STR genotype profile, karyotype, and molecular characterization of SCCOHT-CH-1 cells. BRG1 protein expression in SCCOHT-CH-1, COV434, and IOSE80 cells by western blot.

Northern blotting

Following similar principles to Western blotting, Northern blotting allows scientists to separate RNA molecules on a denaturing gel according to their size (92). The RNA bands are then transferred to a membrane, labeled with complementary probes, and analyzed using a scanner, such as the Amersham Typhoon imager. It enables researchers to study gene expression through quantification of the type and abundance of RNA in a sample. Northern blotting assays employing Amersham Typhoon imagers have contributed to many impactful research studies spanning the fields of plant biology, mitochondrial biology, virology, and genomics.

One such study, recently published in Nature, aimed to investigate the structural basis of ribosomal 30S subunit degradation by RNase R (22). The researchers used an Amersham Typhoon imager to analyze Northern blots of RNA extracted from RNase R immunoprecipitations, which supported the identification and characterization of RNA species and provided insights into RNA degradation processes. Through this, the authors identified a 16S rRNA species truncated by around 150 nucleotides, mapping the truncation site to specific regions of the 16S rRNA and revealing the structural bases of ribosomal 30S subunit degradation. These findings contribute to the knowledge of RNA degradation pathways and the role of RNase R in ribosomal RNA processing and quality control, ultimately representing a pivotal advancement in molecular and structural biology.

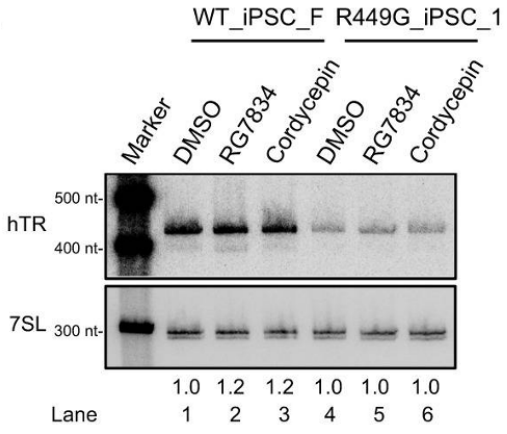

Fig 4. Adapted from Fig 6A (22). Polysome analysis of wild-type and Δrnr strains grown to late-exponential phase. Northern blot analysis of the RNA extracted from gradient fractions with probes against the mature and pre-16S rRNA. The input was stained with Serva stain G. Total RNA from the input lysates and the ΔyqeH strain was used as control. 1 ug of RNA was loaded in all lanes (n = 2). For gel source data, see supplementary Fig. 1.

Applying genomic knowledge to agricultural practices is essential for developing sustainable farming practices, an important and urgent feat in the context of the current threats to food security (93, 94). A recent study by Kumar and colleagues developed an efficient, reproducible in vitro regeneration and transformation protocol for tropical maize using mature seed-derived nodal explants, with the potential to improve maize cultivation through transgenic and genome editing methodologies (15). In this study, the researchers used Northern blotting to analyze the transgenic status of healthy putative transformants, using an Amersham Typhoon imager for visualization.

Finally, Northern blotting has played a pivotal role in efforts to better understand rare diseases. Hoyeraal-Hreidarsson syndrome (HHS) is a rare X-linked recessive disorder caused by mutations in telomere maintenance genes (95). By combining single-cell RNA sequencing, Western blotting, and Northern blotting, researchers uncovered new insights into patient immunodeficiency and shed light on potential treatment options for HHS and other telomerase insufficiency disorders (16).

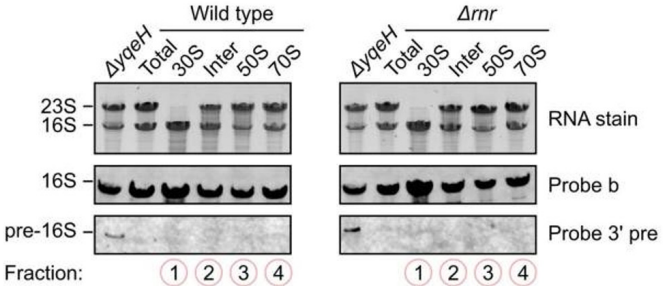

Fig 5. Adapted from Fig 6A (16). Inhibition of oligoadenylation of hTR restores telomerase activity and telomere length in DKC1 mutant iPSCs. Northern blot analysis of hTR from WT_iPSC_F, R449G_iPSC_1, and R449G_iPSC_2 cells treated with RG7834, Cordycepin, or DMSO. A probe against 7SL RNA served as a loading control.

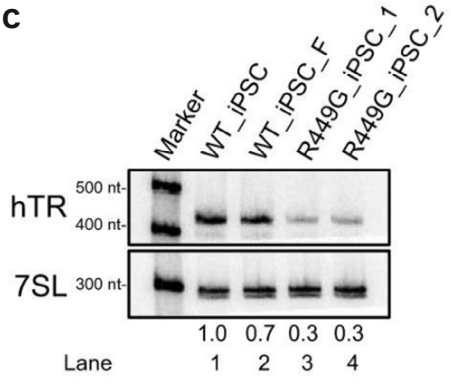

Fig 6. Adapted from Fig 5C (16). DKC1_R449G iPSCs exhibit a shorter telomere length, decreased levels of hTR, reduced telomerase activity, and mislocalized DKC1. Northern blot analysis of hTR from WT_iPSC, WT_iPSC_F, R449G_iPSC_1, and R449G_iPSC_2 cells. A probe against 7SL RNA served as a loading control.

Southern blotting

Southern blotting follows the same principles as Western and Northern blotting to facilitate the detection and quantification of specific DNA sequences (96). Purified, restriction-enzyme digested DNA fragments are separated based on their size on an agarose gel before being transferred to a membrane, labeled with a radioactive, chemical, or fluorescent probe, and imaged with an analyzer like an Amersham Typhoon imager. Southern blotting can be especially useful for examining whether a gene is amplified, deleted, or structurally rearranged in diseased cells, like cancer cells, compared to healthy, age-matched control cells (97).

In a 2023 study from the University of Zurich, the authors aimed to investigate how the interferon (IFN)-mediated inflammatory response regulates DNA replication and repair processes, potentially impacting cancer cell fitness and therapy responses (26). The results, elucidated by Southern blot visualization using an Amersham Typhoon imager, shed light on the essential role of specific genes in IFNβ-mediated viability rescue in BRCA deficient cells, pinpointing it as a critical factor to consider when developing chemotherapeutic and immunotherapeutic strategies.

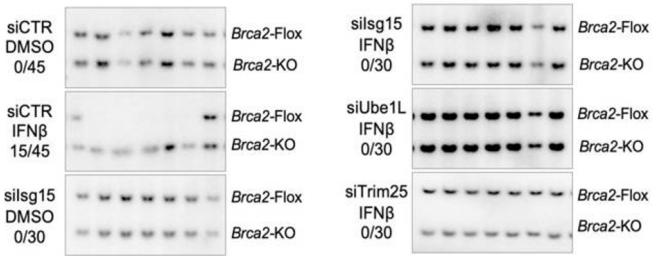

Fig 7. Adapted from Fig 4E (26). Upregulation of IFNβ/ISG15 restores viability in BRCA2-deficient mESCs. Ratio of number of rescued clones and total numbers of HAT-resistant clones analyzed, and representative Southern blot showing Brca2flox/- or Brca2-/- mESC upon ± IFNβ (30 U/mL, 2 h) pre-treatment along with depletion of ISG15, UBE1L or TRIM25 by siRNA treatment.

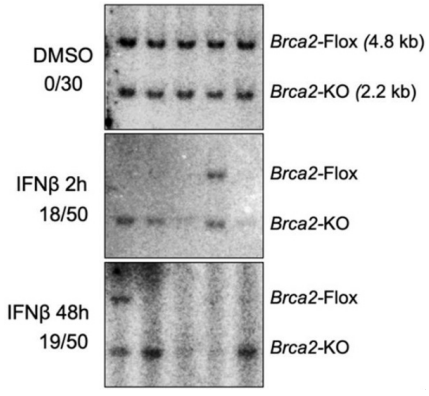

Fig 8. Adapted from Fig 4D (26). Upregulation of IFNβ/ISG15 restores viability in BRCA2-deficient mESCs. Percentage of Brca2-/- HAT resistant clones and representative Southern blot showing Brca2flox/- or Brca2-/- mESC upon ± IFNβ pre-treatment as in (b).

Aside from its essential role in oncology studies, Southern blotting is a crucial component of the molecular biology toolbox. In a recent study investigating the competition between different DNA repair pathways at Cas9-induced DNA double-strand breaks, Southern blotting was used to analyze genomic DNA fragments (24). This led to significant findings that provided key insights into the interplay between DNA repair pathways, with implications for our understanding of genomic stability, instability, and related disease pathways, as well as for genome editing using breakthrough tools like CRISPR-Cas9 (98).

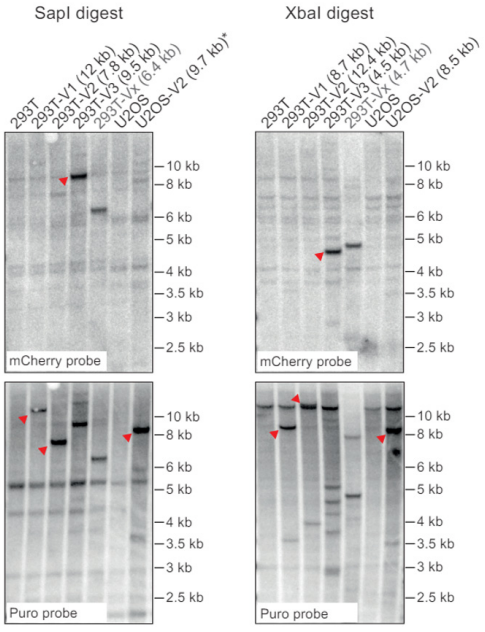

Fig 9. Adapted from Sup Fig 2B (24). Identification and validation of DSB-Spectrum genomic integration sites, Genomic DNA isolated from clonal DSB-Spectrum reporter cell-lines, as well as the parental HEK 293T and U2OS cell-lines as a control, was digested overnight with either SapI or XbaI restriction enzyme, followed by Southern blot analysis as indicated in the methods section.

The blot was hybridized with a probe binding to the puromycin resistance cassette (puro probe) present in DSB-Spectrum variants V1 and V2, followed by stripping and re-hybridization with a probe binding to the mCherry gene (mCherry probe), present in DSB-Spectrum_V3. The sample loaded in lane 5 contains digested DNA from a HEK 293T cell-line containing a DSB-Spectrum variant that was discontinued and not described in the manuscript (293T-Vx). The expected size, based on the Splinkerette results, of the genomic DNA digestion product containing the DSB-Spectrum-derived puromycin resistance or mCherry gene is indicated in brackets behind the labels. Red arrows point towards the products specific for the DSB-Spectrum cell-lines compared to the parental control cell-lines.
An asterisk indicates that the U2OS DSB-Spectrum_V2 cells were double digested with PacI in combination with XbaI.
The data shown are representative of results obtained from five independently performed Southern blots.

Thin layer chromatography

Thin layer chromatography (TLC) is a technique used to separate and identify the components of a mixture based on their polarity via their relative affinities for the stationary or mobile phase. Following TLC separation, the separated compounds are transferred onto a membrane, which can be visualized with a Typhoon scanner. TLC allows scientists to easily separate a mixture into its chemical components, supporting the isolation of components or assessment of the sample's purity. TLC is a versatile technique used across research and industrial applications, such as pharmaceutical production, clinical analysis, and environmental toxicology (99). The application of TLC to major scientific research questions is exemplified in a 2023 Nature Communications publication by Brkic et al. (34). In this study, the authors aimed to investigate antibiotic hyper-resistance in a class I aminoacyl-tRNA synthetase with an altered active site signature motif. By applying TLC, along with other innovative structural modeling and molecular dynamics simulations, they were able to detail the structural basis of mupirocin resistance and elucidate a mechanism of hyper-resistance. This study, which used a Typhoon scanner for TLC imaging and ImageQuant™ TL software for data analysis, carries significant implications not only for research but for society as a whole, given that antimicrobial resistance remains one of the greatest threats to global health (100).

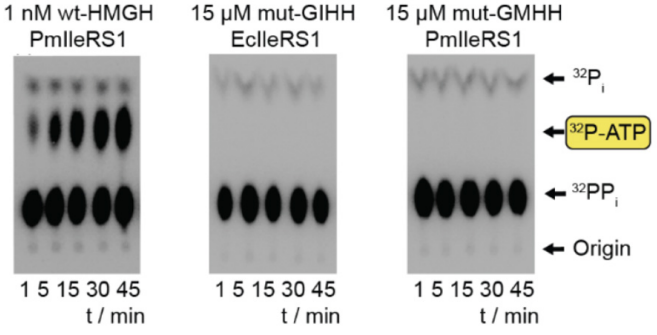

Fig 10. Adapted from Sup Fig 3 (34). Stability of [18F]TPF in human serum. Thin-layer chromatograms showing the lack of 32P-ATP formation by the GXHH-IleRS1 enzymes present at high concentrations (15 mM) and prolonged reaction times. 1 nM wt PmIleRS1 was used as a positive control.

TLC is been widely used in several studies that aimed to develop innovative tools for clinical use. For example, one such study applied TLC to characterize a fluorescin-based 18F-tracer for pre-targeted positron emission tomography (PET) imaging (29). Here, TLC analysis was applied to assess the stability and capture of [18F]TPF, and images were visualized using a Typhoon scanner, which supported the feasibility of [18F]TPF as a new tracer for clinical visualization of disease-specific processes via PET imaging. In addition to this study, numerous other studies, highlighted in Table 1, applied the Typhoon Imager to radioactive probe development for diagnostic purposes.

Fig 11. Adapted from Sup Fig 8 (29). Stability of [18F]TPF in human serum

Phosphor imaging

Phosphor imaging is a technique that uses photostimulable phosphor plates to detect and quantify radioactive signals from biological samples, such as in Western blotting experiments. It is an advanced alternative to X-ray film autoradiography, a technique that has been widely used by scientists for many years. Phosphor imaging significantly reduces exposure time, has far higher sensitivity, and has a broader dynamic range than conventional X-ray film-based autoradiography, allowing researchers to obtain more robust data across various scientific imaging applications (101). In genomics, phosphor imaging, with highly sensitive, high-throughput scanners like the Typhoon series, is used alongside techniques like next-generation sequencing (NGS) due to its high sensitivity and ability to detect trace amounts of radiolabelled nucleotides.

For example, in virology, phosphor imaging with Amersham Typhoon scanners has been applied to answer research questions on influenza and SARS-CoV-2 viruses. One publication used phosphor imaging to detect phosphorylation of the PA subunit of the influenza polymerase (60). The findings of this study highlighted the functional relevance of PA phosphorylation in controlling viral polymerase activity during the influenza infectious cycle, which may have important implications for population health efforts and the development of safe and effective vaccines.

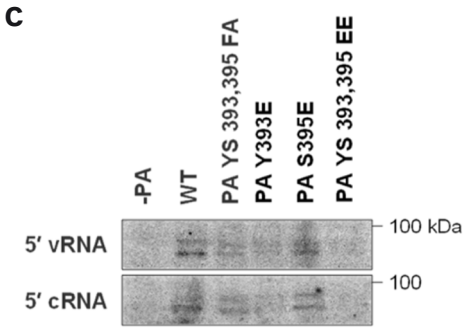

Fig 12. Adapted from Fig 4C (60). PA Y393 phosphorylation prevents polymerase binding to the 5′-termini of vRNA and cRNA. The purified polymerase was incubated with the radiolabeled 5′ ends of vRNA or cRNA in the presence of their respective unlabeled 3′ promoters. After UV crosslinking the RNA/polymerase complex, the proteins were resolved by SDS-PAGE and the dried gel was analyzed by phosphorimaging.

In another virology paper aimed at investigating the impact of SARS-CoV-2 pathogenesis on lung tissue translational regulation, researchers applied ribosome profiling to analyze ribonucleoprotein interactions and translation profiles in infected lung tissues, using an Amersham Typhoon imager to accurately visualize radioisotope signals (62). This work highlighted the critical role of translation integrity in contributing to tissue pathogenesis after SARS-CoV-2 infection. Together, these high-impact virology studies showcase the versatile role of phosphor imaging with Amersham Typhoon scanners in contributing to research efforts surrounding significant global health challenges.

Electrophoretic mobility shift assay

The gel electrophoretic mobility shift assay (EMSA) is used to detect interactions between proteins and nucleic acids. It involves separating samples via native gel electrophoresis, based on the assumption that protein-nucleic acid complexes migrate more slowly than the corresponding free nucleic acid. Then, the identification of protein-nucleic acid complexes is determined, usually via autoradiography, using a scanner like the Typhoon series scanners, to detect 32P-labeled nucleic acids (102). In EMSA, the large scan area of Typhoon imagers is particularly beneficial due to the large gels used, allowing researchers to resolve more bands.

A 2023 Nature Communications publication applied EMSA to investigate the role of endogenous S-nitrosylation in regulating vancomycin resistance in S. aureus (67). Vancomycin is used as a 'last-resort' treatment in patients with severe infections that have not responded to other antibiotics, such as MRSA. Therefore, resistance to vancomycin can have catastrophic consequences, and we urgently need to understand resistance mechanisms in order to develop better treatment strategies (103). By applying EMSA and detecting band shifts using an Amersham Typhoon scanner with ImageQuant TL software for analysis, among other techniques, the authors demonstrated that endogenous S-nitrosylation plays a crucial role in vancomycin resistance, providing clinically meaningful insights relevant to the treatment of antibiotic-resistant pathogens.

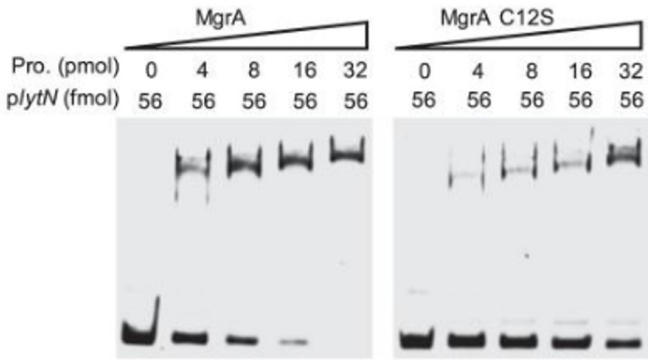

Fig 13. Adapted from Fig 5E (67). Removal of MgrA S-nitrosylation impairs its DNA binding activity. DNA binding efficacy of WT and C12S mutant MgrA at lytN (e) or sarV (f) promoters was compared by using gel-shift assay.

Another clinically relevant immunology study used EMSA to analyze B cell receptor-antigen binding, elucidating an activation mechanism determined by the antigen footprint that may influence future therapeutic strategies (64).

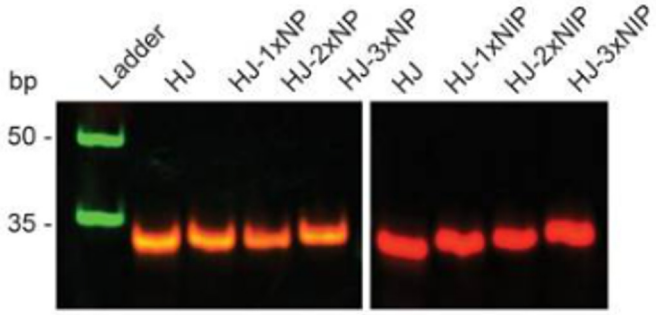

Fig 14. Adapted from Fig 2C (64). Assembly of hapten-functionalized HJs and their binding profile to B1-8 anti-NP mAb. Native PAGE gel showing the assembly of HJs carrying up to three NP/NIP conjugates and a Q2 oligo bearing AF647 for detection. Green signal is SYBR Gold stain and red signal is AF647. Size marker used is an ultra-low range DNA ladder.

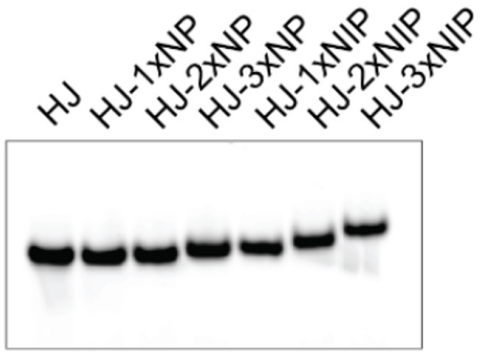

Fig 15. Adapted from Sup Fig 6A ref (64). Flow-induced dispersion analysis (FIDA) of HJ-NIP constructs. A 12% native PAGE gel of Atto488-modified HJs displaying 0-3 units of NP or NIP used in FIDA analysis. As this is native PAGE, it was not possible to include a meaningful molecular weight marker. Experiment was repeated independently at least two times with similar results.

In addition to phosphor imaging and EMSA, their high sensitivity and ability to generate accurate, robust data make Typhoon scanners the gold standard imager used in quantitative whole-body autoradiography (QWBA), which biopharmaceutical companies use to study compound tissue distribution (104).

Stain, dye based gel, and plate visualization

The gel electrophoretic mobility shift assay (EMSA) is used Colorimetric imaging is a technique that uses color changes to detect and quantify the presence of specific analytes or substances. Similarly, stains or dyes can be combined with fluorescence-based imaging to achieve the same result. Commonly used stains for colorimetric imaging include Coomassie blue dyes, used to detect proteins in polyacrylamide gels (105), and silver staining, a less widely used method of protein detection with higher sensitivity than Coomassie staining (106). Meanwhile, the detection of nucleic acids can be achieved using SYBR Gold staining (107), while phosphorylated proteins can be detected using stains like the Pro-Q Diamond Phosphoprotein Gel Stain (108).

For example, in a recent plant biology study investigating changes in tomato resistance mechanisms and the interplay of crucial signaling cascades, the researchers applied Pro-Q Diamond staining, imaged using a Typhoon scanner, to detect phosphorylated proteins central to signaling cascade activation and signal transduction (78).

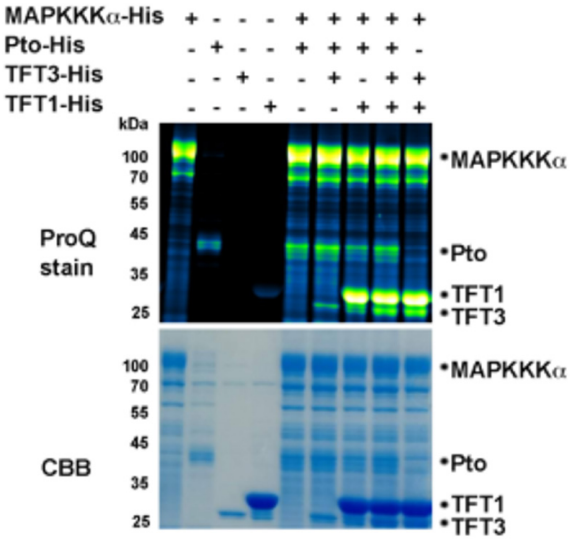

Fig 16. Adapted from Sup Fig 7a ref (78). Phosphorylation dynamics of Prf/Pto components. Kinase activity assay showing the phosphorylation status of MAPKKKa in vitro. Purified His-tagged proteins (MAPKKKa, Pto, TFT1, and TFT3) were incubated in the indicated combinations in a kinase buffer. The proteins were separated on a 10% SDS-PAGE gel and stained with ProQ Diamond stain which specifically stains phosphorylated proteins (bright green/blue bands). Coomassie Brilliant Blue (CBB) staining of the SDS-PAGE gels was used to verify protein loading.

Meanwhile, in a study conducted at the University of Copenhagen, scientists aimed to investigate the genetic vulnerabilities to inhibition of SUMOylation in human cells in order to better understand the potential of SUMO modification as a potential strategy for cancer treatment (80). Here, SUMOylation assays were visualized through Coomassie staining with a Typhoon scanner. Protein stains such as Coomassie and silver staining can also be used to visualize the results of two-dimensional gel electrophoresis (2D-GE). 2D-GE facilitates the comparison of protein complexes by first separating them by their isoelectric point (pI) and then by their molecular weight before staining and visualizing bands using an imager such as a Typhoon scanner (109).

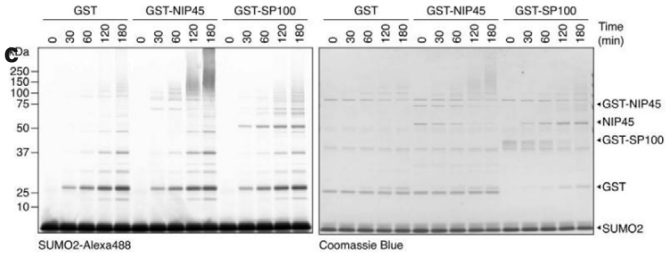

Fig 17. Adapted from figure extended data Fig 7c (80). NIP45 stimulates SUMO modification and interacts with SLX4. In vitro SUMO modification assays containing purified SAE1/SAE2, UBC9, Alexa 488-labeled SUMO1 (b) or SUMO2 (c) and either GST, GST-NIP45 or GST-SP100(241-360) were incubated at 37 °C for the indicated time. Reaction products were analyzed by SDS-PAGE and visualized by fluorescent scanning to detect Alexa 488 (left panel) or Coomassie blue staining (right panel).

The versatility of stain-based imaging means that, aside from its important research implications, it can be applied to complex translational questions, such as in developing drug delivery mechanisms. In a study by Velusamy et al., DNA mechanocapsules (DMCs) were investigated as a method of drug delivery (85). In this study, agarose gels were stained with SYBR Gold and imaged using Typhoon scanners to facilitate the visualization of DNA structures, a central component of this study. The study highlighted the potential of DMCs as a programmable, piconewton-responsive drug delivery system with therapeutic applications in immunology and cancer biology.

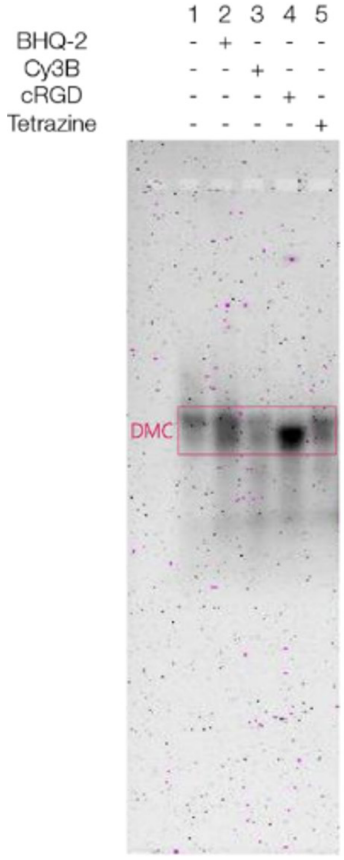

Fig 18. Adapted from supplementary Fig 7c (85). Characterization of DMC formation. b DMC with various chemical modifications at 50 nM concentrations. DMCs fold with high yield (>95%) when annealed at lower concentrations.

In addition to the staining of gels and membranes, many plant studies use Typhoon RGB imagers to visualize fluorescence directly in plant tissues, exemplifying its versatility not only across different applications but also in various sample types. Similarly, Typhoon imagers are ideal for directly evaluating autofluorescence or fluorescent proteins.

Two-Dimensional Differential In-Gel Electrophoresis (2D DIGE)

2D DIGE is a technique used in proteomics research to compare protein expression patterns among different samples. It involves labelling proteins from various samples with different fluorescent dyes, Cy2, Cy3 and Cy5, and then mixing the samples together. The labeled proteins are then separated by 2D gel electrophoresis based on their isoelectric point (pI) and molecular weight. After gel electrophoresis, the gel is scanned to detect the fluorescent signals from the labeled proteins, and the intensity of the signals is used to quantify the relative abundance of proteins in the different samples. DIGE allows for the simultaneous analysis of multiple samples on the same gel, reducing experimental variability and enabling accurate protein expression comparisons.

The authors employ 2D-DEGE to analyze the charge variants of biosimilars, which are gaining economic importance and reducing healthcare costs worldwide. Determining the similarity between a biosimilar and its originator has traditionally been done on a case-by-case basis both in the scientific protein characterization and in the regulatory framework.

In this study, the authors shed light on charge heterogeneity, a frequently cited critical quality attribute of monoclonal antibodies. By utilizing a high-resolution 2D DIGE method, they are able to visualize, separate, and quantify the charge variant profiles of the originator monoclonal antibody (in this case, infliximab) and three biosimilars. This unique approach allows for the elucidation of similarities among multiple biosimilars and their originator by accurately analyzing charge variants. Additionally, the authors complement their findings with chromatographic analysis and Biacore(TM) SPR system binding assays to comprehensively characterize the similarities between the originator and its biosimilars.

Amersham Typhoon scanners: Features and benefits

As highlighted in the applications we have discussed, the Amersham Typhoon biomolecular imagers are highly versatile, advanced laser scanners engineered for flexible imaging and accurate quantification of fluorescent, colorimetric, and radiolabeled proteins and nucleic acids. We understand the ever-changing nature of the research laboratory and the need for flexibility, and we integrated this into the modular, customizable design of the Amersham Typhoon imagers. The Typhoon scanner series comprises five different configurations to meet the needs of various research labs (Table 2). The key benefits of Typhoon scanners, exemplified in the publications discussed, are explored in detail in the following sections.

High sensitivity and enhanced dynamic range

State-of-the-art lasers and photomultiplier detectors are at the heart of the Amersham Typhoon imager design, resulting in unparalleled sensitivity and an extensive dynamic range. These features are crucial across fundamental, translational, and clinical research, where detecting low levels of biomolecules or discerning minute differences between samples with precision can lead to important insights. The linear signal response, quantitative accuracy, and exceptionally low detection limits support the generation of robust data with unmatched quality. The systems' dynamic range, extending over five orders of magnitude, further enhances the capacity for sensitive and accurate protein quantification.

Flexible, modular design

The Amersham Typhoon 5 imager integrates the capabilities of four instruments into a single modular platform that can be customized to meet the changing needs of evolving research projects. The system supports various imaging modes: near-infrared (NIR) fluorescence, RGB fluorescence, phosphor imaging, and densitometry for colorimetrically stained samples (Table 2). Moreover, its customizable features allow researchers to select optimal laser configurations for RGB or NIR detection.

High sample throughput

The Amersham Typhoon scanners provide researchers with a high sample throughput capacity, facilitated by the large 40 × 46 cm scanning area. This scanning area size allows for the simultaneous imaging of up to 20 gels or blots (typically 10 × 8 cm) or up to nine multiwell plates in a single scan. This high-throughput capacity significantly reduces workload and waiting times for researchers, boosting laboratory productivity. Furthermore, the large scan area and multi-channel fluorescence capabilities are ideal for investigating samples with fluorescent proteins, and in many cases, the autofluorescence of biological samples can also be measured at high resolution.

Quick and easy-to-use

Amersham Typhoon imagers have automatic filter recognition and auto- and semi-auto-scan functions that support robust data generation in just three clicks, enabling fast and easy use with minimal training.

Image integrity

The journey to robust data doesn't stop once you have imaged your get, blot, or plate. We offer image analysis and verification solutions compatible with Typhoon scanners. The ImageQuant TL analysis software allows users to reliably analyze gel and blot images using band detection, background subtraction, and lane comparison tools. Its quantity calibration and normalization tools eliminate the risk of calculation errors and support consistency between analyses. Following analysis, our Image Integrity Checker enables researchers to check if an image generated with Amersham Typhoon systems has been modified. This streamlines the verification process, offering a rapid assessment of image authenticity that ensures researchers do not waste time inadvertently analyzing a manipulated image.

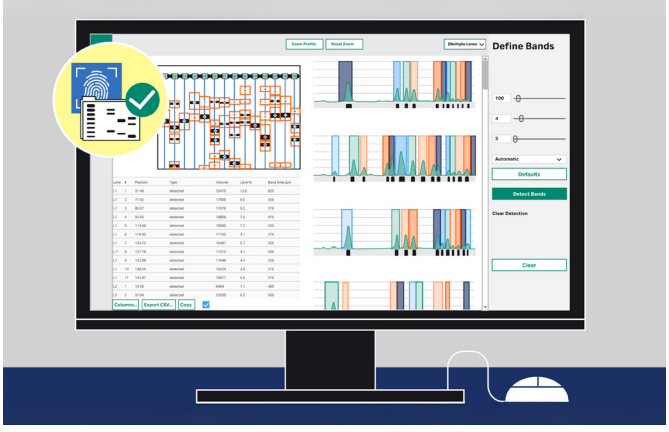

Fig 19. Illustration of ImageQuant TL analysis and Image integrity checker software.

Table 2. Estimated Configurations and capabilities of the Typhoon scanner series. X = supported, O = not supported. OD = optical density.
(1) An OD plate is needed. (2) Only the green fluorescence channel is included.

	Phosphor Imaging	Densitometry (OD)	RGB Fluorescence	Near-Infrared Fluorescence
Amersham Typhoon IP	X	O	O	O
Amersham Typhoon NIR	O	O	O	X
Amersham Typhoon NIR Plus	O	X (1)	X (2)	X
Amersham Typhoon RGB	X	X	X	O
Amersham Typhoon 5	X	X	X	X

Conclusion

This comprehensive review of Amersham Typhoon biomolecular imagers has demonstrated their role in advancing life sciences research. From providing unparalleled sensitivity in detecting biomolecules to offering a versatile platform for a wide range of applications, the Amersham Typhoon scanners have proven to be indispensable tools in research and industrial applications. Whether it's elucidating the molecular basis of diseases like Parkinson's, advancing our knowledge of RNA degradation and DNA replication mechanisms, or pioneering new methods for studying drug resistance and delivery, these scanners are integral to facilitating accurate, efficient, and robust biomolecular imaging. The devices' high sensitivity, enhanced dynamic range, flexible modular design, and high-throughput capabilities have facilitated not only the generation of robust data but also the exploration of complex biological questions across various research areas. The reviewed publications showcase the Amersham Typhoon scanner series' applications in neurobiology, structural biology, oncology, microbiology, virology, molecular biology, plant biology, and drug discovery, highlighting its instrumental role in advancing scientific discovery. To find out more about how Amersham Typhoon scanners can support your research goals, request a quote today. One of our imaging specialists will get in touch.

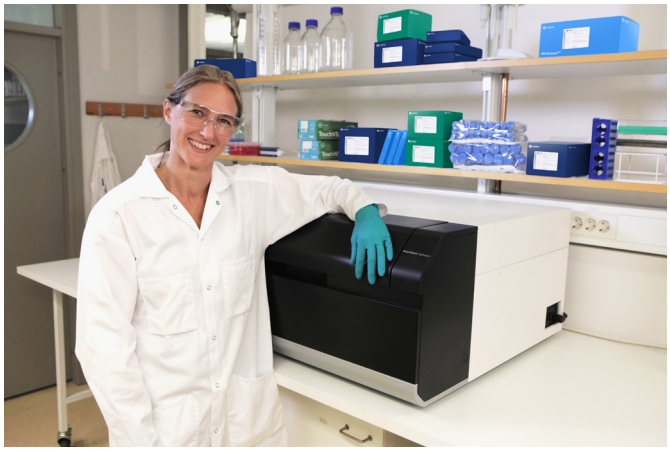

References citing the use of Amersham Typhoon laser scanner

1. Szaniszló T, Fülöp M, Pajkos M, Erdős G, Kovács RÁ, Vadászi H, et al. The interaction between LC8 and LCA5 reveals a novel oligomerization function of LC8 in the ciliary-centrosome system. Sci Rep. 2022 Sep 16;12(1):15623.
2. Matalkah F, Jeong B, Sheridan M, Horstick E, Ramamurthy V, Stoilov P. The Musashi proteins direct post-transcriptional control of protein expression and alternate exon splicing in vertebrate photoreceptors. Commun Biol. 2022 Sep 24;5(1):1011.
3. Wang SH, Cheng JY, Tsai HH, Lo TC, Hung JT, Lin CC, et al. Conformational alteration in glycan induces phospholipase Cβ1 activation and angiogenesis. J Biomed Sci. 2022 Dec 15;29(1):105.
4. Chen J, Chen M, Zhu TF. Directed evolution and selection of biostable l-DNA aptamers with a mirror-image DNA polymerase. Nat Biotechnol. 2022 Nov;40(11):1601–9.
5. Drobny A, Boros FA, Balta D, Prieto Huarcaya S, Caylioglu D, Qazi N, et al. Reciprocal effects of alpha-synuclein aggregation and lysosomal homeostasis in synucleinopathy models. Transl Neurodegener. 2023 Jun 13;12(1):31.
6. Yang G, Kantapan J, Mazhar M, Bai X, Zou Y, Wang H, et al. Mesenchymal stem cells transplantation combined with IronQ attenuates ICH-induced inflammation response via Mincle/syk signaling pathway. Stem Cell Res Ther. 2023 May 15;14(1):131.
7. Martin S, Allan KC, Pinkard O, Sweet T, Tesar PJ, Coller J. Oligodendrocyte differentiation alters tRNA modifications and codon optimality-mediated mRNA decay. Nat Commun. 2022 Aug 25;13(1):5003.
8. Gao Y, Zheng K, Kang M, Xu J, Ning Y, Hu W, et al. Establishment and characterization of a novel cell line (SCCOHT-CH-1) and PDX models derived from Chinese patients of small cell ovarian carcinoma of the hypercalcemic type. Hum Cell. 2023 Aug 3;36(6):2214–27.
9. Peeters R, Cuenca-Escalona J, Zaal EA, Hoekstra AT, Balvert ACG, Vidal-Manrique M, et al. Fatty acid metabolism in aggressive B-cell lymphoma is inhibited by tetraspanin CD37. Nat Commun. 2022 Sep 13;13(1):5371.
10. Liu XZ, Rulina A, Choi MH, Pedersen L, Lepland J, Takle ST, et al. C/EBPB-dependent adaptation to palmitic acid promotes tumor formation in hormone receptor negative breast cancer. Nat Commun. 2022 Jan 10;13(1):69.
11. Li Y, Niu Z, Yang J, Yang X, Chen Y, Li Y, et al. Rapid metabolic reprogramming mediated by the AMP-activated protein kinase during the lytic cycle of Toxoplasma gondii. Nat Commun. 2023 Jan 26;14(1):422.
12. Fan F, Xue L, Yin X, Gupta N, Shen B. AP2XII-1 is a negative regulator of merogony and presexual commitment in Toxoplasma gondii. Soldati-Favre D, editor. mBio. 2023 Oct 31;14(5):e01785-23.
13. You Y, Koczyk G, Nuc M, Morbitzer R, Holmes DR, Von Roepenack-Lahaye E, et al. The eINTACT system dissects bacterial exploitation of plant osmosignalling to enhance virulence. Nat Plants. 2022 Dec 22;9(1):128–41.
14. Dunkelmann DL, Piedrafita C, Dickson A, Liu KC, Elliott TS, Fiedler M, et al. Adding α,α-disubstituted and β-linked monomers to the genetic code of an organism. Nature. 2024 Jan 18;625(7995):603–10.
15. Kumar K, Jha AK, Kumar B, Karjagi CG, Abhishek A, Gambhir G, et al. Development of an efficient and reproducible in vitro regeneration and transformation protocol for tropical maize (Zea mays L.) using mature seed-derived nodal explants. Plant Cell Tissue Organ Cult PCTOC. 2022 Mar;148(3):557–71.
16. Chu CM, Yu HH, Kao TL, Chen YH, Lu HH, Wu ET, et al. A missense variant in the nuclear localization signal of DKC1 causes Hoyeraal-Hreidarsson syndrome. Npj Genomic Med. 2022 Oct 30;7(1):64.
17. Sharma S, Yang J, Favate J, Shah P, Kiledjian M. NADcapPro and circNC: methods for accurate profiling of NAD and non-canonical RNA caps in eukaryotes. Commun Biol. 2023 Apr 13;6(1):406.
18. Huber M, Lippegaus A, Melamed S, Siemers M, Wucher BR, Hoyos M, et al. An RNA sponge controls quorum sensing dynamics and biofilm formation in Vibrio cholerae. Nat Commun. 2022 Dec 8;13(1):7585.
19. Sharma S, Yang J, Grudzien-Nogalska E, Shivas J, Kwan KY, Kiledjian M. Xrn1 is a deNADding enzyme modulating mitochondrial NAD-capped RNA. Nat Commun. 2022 Feb 16;13(1):889.
20. Leister D, Sharma A, Kerber N, Nägele T, Reiter B, Pasch V, et al. An ancient metabolite damage-repair system sustains photosynthesis in plants. Nat Commun. 2023 May 25;14(1):3023.
21. Kumar J, Kumar RR, Das DK, Mohanty A, Rajani K, Kumari N, et al. Knockdown of capsid protein encoding novel ATPase domain inhibits genome packaging in potato leafroll virus. 3 Biotech. 2022 Mar;12(3):66.
22. Dimitrova-Paternoga L, Kasvandik S, Beckert B, Granneman S, Tenson T, Wilson DN, et al. Structural basis of ribosomal 30S subunit degradation by RNase R. Nature. 2024 Feb 29;626(8001):1133–40.
23. Dremel SE, Sivrich FL, Tucker JM, Glaunsinger BA, DeLuca NA. Manipulation of RNA polymerase III by Herpes Simplex Virus-1. Nat Commun. 2022 Feb 2;13(1):623.
24. Van De Kooij B, Kruswick A, Van Attikum H, Yaffe MB. Multi-pathway DNA-repair reporters reveal competition between end-joining, single-strand annealing and homologous recombination at Cas9-induced DNA double-strand breaks. Nat Commun. 2022 Sep 8;13(1):5295.

25. Joseph CR, Dusi S, Giannattasio M, Branzei D. Rad51-mediated replication of damaged templates relies on monoSUMOylated DDK kinase. Nat Commun. 2022 May 5;13(1):2480.
26. Moro RN, Biswas U, Kharat SS, Duzanic FD, Das P, Stavrou M, et al. Interferon restores replication fork stability and cell viability in BRCA-defective cells via ISG15. Nat Commun. 2023 Oct 2;14(1):6140.
27. Bedard MC, Chihanga T, Carlile A, Jackson R, Brusadelli MG, Lee D, et al. Single cell transcriptomic analysis of HPV16-infected epithelium identifies a keratinocyte subpopulation implicated in cancer. Nat Commun. 2023 Apr 8;14(1):1975.
28. Prasad A, Prasad M. Interaction of ToLCNDV TrAP with SlATG8f marks it susceptible to degradation by autophagy. Cell Mol Life Sci. 2022 May;79(5):241.
29. Helbert H, Ploeg EM, Samplonius DF, Blok SN, Antunes IF, Böhmer VI, et al. A proof-of-concept study on the use of a fluorescein-based 18F-tracer for pretargeted PET. EJNMMI Radiopharm Chem. 2022 Mar 3;7(1):3.
30. Pringle TA, Ramon-Gil E, Leslie J, Oakley F, Wright MC, Knight JC, et al. Synthesis and preclinical evaluation of a 89Zr-labelled human single chain antibody for non-invasive detection of hepatic myofibroblasts in acute liver injury. Sci Rep. 2024 Jan 5;14(1):633.
31. Fan X, Ważyńska MA, Kol A, Perujo Holland N, Fernandes B, Van Duijnhoven SMJ, et al. Development of [89Zr]Zr-hCD103.Fab01A and [68Ga]Ga-hCD103.Fab01A for PET imaging to noninvasively assess cancer reactive T cell infiltration: Fab-based CD103 immunoPET. EJNMMI Res. 2023 Nov 20;13(1):100.
32. Mossel P, Arif WM, De Souza GS, Varela LG, Van Der Weijden CWJ, Boersma HH, et al. Quantification of P-glycoprotein function at the human blood-brain barrier using [18F]MC225 and PET. Eur J Nucl Med Mol Imaging. 2023 Nov;50(13):3917–27.
33. Lemm S, Köhler S, Wodtke R, Jung F, Küpper JH, Pietzsch J, et al. Investigation of Radiotracer Metabolic Stability In Vitro with CYP-Overexpressing Hepatoma Cell Lines. Cells. 2022 Aug 7;11(15):2447.
34. Brkic A, Leibundgut M, Jablonska J, Zanki V, Car Z, Petrovic Perokovic V, et al. Antibiotic hyper-resistance in a class I aminoacyl-tRNA synthetase with altered active site signature motif. Nat Commun. 2023 Sep 7;14(1):5498.
35. Blumenreich S, Nehushtan T, Kupervaser M, Shalit T, Gabashvili A, Joseph T, et al. Large-scale proteomics analysis of five brain regions from Parkinson's disease patients with a GBA1 mutation. Npj Park Dis. 2024 Feb 8;10(1):33.
36. Glynos NG, Carter L, Lee SJ, Kim Y, Kennedy RT, Mashour GA, et al. Indolethylamine N-methyltransferase (INMT) is not essential for endogenous tryptamine-dependent methylation activity in rats. Sci Rep. 2023 Jan 6;13(1):280.
37. Chandana M, Anand A, Ghosh S, Das R, Beura S, Jena S, et al. Malaria parasite heme biosynthesis promotes and griseofulvin protects against cerebral malaria in mice. Nat Commun. 2022 Jul 12;13(1):4028.
38. Zelnik ID, Mestre B, Weinstein JJ, Dingjan T, Izrailov S, Ben-Dor S, et al. Computational design and molecular dynamics simulations suggest the mode of substrate binding in ceramide synthases. Nat Commun. 2023 Apr 22;14(1):2330.
39. Pitsawong W, Pádua RAP, Grant T, Hoemberger M, Otten R, Bradshaw N, et al. From primordial clocks to circadian oscillators. Nature. 2023 Apr 6;616(7955):183–9.
40. Silva-Pinheiro P, Mutti CD, Van Haute L, Powell CA, Nash PA, Turner K, et al. A library of base editors for the precise ablation of all protein-coding genes in the mouse mitochondrial genome. Nat Biomed Eng. 2022 Dec 5;7(5):692–703.
41. Durand S, Bruelle M, Bourdelais F, Bennychen B, Blin-Gonthier J, Isaac C, et al. RSL24D1 sustains steady-state ribosome biogenesis and pluripotency translational programs in embryonic stem cells. Nat Commun. 2023 Jan 23;14(1):356.
42. Levina A, Fleming KD, Burke JE, Leonard TA. Activation of the essential kinase PDK1 by phosphoinositide-driven trans-autophosphorylation. Nat Commun. 2022 Apr 6;13(1):1874.
43. Umanah GKE, Abalde-Atristain L, Khan MR, Mitra J, Dar MA, Chang M, et al. AAA + ATPase Thorase inhibits mTOR signaling through the disassembly of the mTOR complex 1. Nat Commun. 2022 Aug 17;13(1):4836.
44. Pellico J, Vass L, Carrascal-Miniño A, Man F, Kim J, Sunassee K, et al. In vivo real-time positron emission particle tracking (PEPT) and single particle PET. Nat Nanotechnol [Internet]. 2024 Jan 19 [cited 2024 Apr 11]; Available from: https://www.nature.com/articles/s41565-023-01589-8
45. Kim Y il, Lee SH, Jung JH, Kim SY, Ko N, Lee SJ, et al. 18F-ASEM PET/MRI targeting alpha7-nicotinic acetylcholine receptor can reveal skeletal muscle denervation. EJNMMI Res. 2024 Jan 22;14(1):8.
46. Deshayes S, Baugé C, Dupont PA, Simard C, Rida H, De Boysson H, et al. [18F]FDG PET-MR characterization of aortitis in the IL1rn−/− mouse model of giant-cell arteritis. EJNMMI Res. 2023 Nov 29;13(1):103.
47. Pouyan P, Zemella A, Schloßhauer JL, Walter RM, Haag R, Kubick S. One to one comparison of cell-free synthesized erythropoietin conjugates modified with linear polyglycerol and polyethylene glycol. Sci Rep. 2023 Apr 19;13(1):6394.
48. Clausen AS, Christensen C, Christensen E, Cold S, Kristensen LK, Hansen AE, et al. Development of a 64Cu-labeled CD4+ T cell targeting PET tracer: evaluation of CD4 specificity and its potential use in collagen-induced arthritis. EJNMMI Res. 2022 Sep 16;12(1):62.

49. Liwocha J, Li J, Purser N, Rattanasopa C, Maiwald S, Krist DT, et al. Mechanism of millisecond Lys48-linked poly-ubiquitin chain formation by cullin-RING ligases. Nat Struct Mol Biol. 2024 Feb;31(2):378–89.
50. Yunn NO, Lee J, Lee HS, Oh EJ, Park M, Park S, et al. An aptamer agonist of the insulin receptor acts as a positive or negative allosteric modulator, depending on its concentration. Exp Mol Med. 2022 Apr 27;54(4):531–41.
51. Pike AM, Friend CM, Bell SP. Distinct RPA functions promote eukaryotic DNA replication initiation and elongation. Nucleic Acids Res. 2023 Oct 27;51(19):10506–18.
52. Kang MS, Hamadjida A, Bédard D, Nuara SG, Gourdon JC, Frey S, et al. Distribution of [11C]-JNJ-42491293 in the marmoset brain: a positron emission tomography study. Naunyn Schmiedebergs Arch Pharmacol. 2023 Sep;396(9):2095–103.
53. Vugic D, Dumoulin I, Martin C, Minello A, Alvaro-Aranda L, Gomez-Escudero J, et al. Replication gap suppression depends on the double-strand DNA binding activity of BRCA2. Nat Commun. 2023 Jan 27;14(1):446.
54. Kwon Y, Rösner H, Zhao W, Selemenakis P, He Z, Kawale AS, et al. DNA binding and RAD51 engagement by the BRCA2 C-terminus orchestrate DNA repair and replication fork preservation. Nat Commun. 2023 Jan 26;14(1):432.
55. Ghosh S, Kundu R, Chandana M, Das R, Anand A, Beura S, et al. Distinct evolution of type I glutamine synthetase in Plasmodium and its species-specific requirement. Nat Commun. 2023 Jul 14;14(1):4216.
56. Zhang T, Bai L, Guo Y. SCAB1 coordinates sequential Ca2+ and ABA signals during osmotic stress induced stomatal closure in Arabidopsis. Sci China Life Sci. 2024 Jan;67(1):1–18.
57. Kayzar-Boggs TM, Luitjohan KE, Imhoff SD, Edwards MA, Krajewski KJ, Denton JS, et al. Results from a controlled depleted uranium metal casting experiment designed to investigate nuclear Forensic Radiochronometry Signatures. J Radioanal Nucl Chem. 2023 Jun;332(6):1695–706.
58. Ghanim GE, Sekne Z, Balch S, Van Roon AMM, Nguyen THD. 2.7 Å cryo-EM structure of human telomerase H/ACA ribonucleoprotein. Nat Commun. 2024 Jan 25;15(1):746.
59. Xu L, Liu T, Chung K, Pyle AM. Structural insights into intron catalysis and dynamics during splicing. Nature. 2023 Dec 21;624(7992):682–8.
60. Liu L, Madhugiri R, Saul VV, Bacher S, Kracht M, Pleschka S, et al. Phosphorylation of the PA subunit of influenza polymerase at Y393 prevents binding of the 5l-termini of RNA and polymerase function. Sci Rep. 2023 Apr 29;13(1):7042.
61. Durieux Trouilleton Q, Barata-García S, Arragain B, Reguera J, Malet H. Structures of active Hantaan virus polymerase uncover the mechanisms of Hantaviridae genome replication. Nat Commun. 2023 May 23;14(1):2954.
62. Kim J, Youn D, Choi S, Lee YW, Sumberzul D, Yoon J, et al. SARS-CoV-2 infection engenders heterogeneous ribonucleoprotein interactions to impede translation elongation in the lungs. Exp Mol Med. 2023 Nov 1;55(12):2541–52.
63. Arragain B, Durieux Trouilleton Q, Baudin F, Provaznik J, Azevedo N, Cusack S, et al. Structural snapshots of La Crosse virus polymerase reveal the mechanisms underlying Peribunyaviridae replication and transcription. Nat Commun. 2022 Feb 16;13(1):902.
64. Ferapontov A, Omer M, Baudrexel I, Nielsen JS, Dupont DM, Juul-Madsen K, et al. Antigen footprint governs activation of the B cell receptor. Nat Commun. 2023 Feb 22;14(1):976.
65. Wang W, Götte B, Guo R, Pyle AM. The E3 ligase Riplet promotes RIG-I signaling independent of RIG-I oligomerization. Nat Commun. 2023 Nov 11;14(1):7308.
66. Lee TA, Han H, Polash A, Cho SK, Lee JW, Ra EA, et al. The nucleolus is the site for inflammatory RNA decay during infection. Nat Commun. 2022 Sep 3;13(1):5203.
67. Shu X, Shi Y, Huang Y, Yu D, Sun B. Transcription tuned by S-nitrosylation underlies a mechanism for Staphylococcus aureus to circumvent vancomycin killing. Nat Commun. 2023 Apr 21;14(1):2318.
68. Yang R, Shi Q, Huang T, Yan Y, Li S, Fang Y, et al. The natural pyrazolotriazine pseudoiodinine from Pseudomonas mosselii 923 inhibits plant bacterial and fungal pathogens. Nat Commun. 2023 Feb 9;14(1):734.
69. Damke PP, Celma L, Kondekar SM, Di Guilmi AM, Marsin S, Dépagne J, et al. ComFC mediates transport and handling of single-stranded DNA during natural transformation. Nat Commun. 2022 Apr 12;13(1):1961.
70. Jaiswal RK, Lei KH, Chastain M, Wang Y, Shiva O, Li S, et al. CaMKK2 and CHK1 phosphorylate human STN1 in response to replication stress to protect stalled forks from aberrant resection. Nat Commun. 2023 Nov 30;14(1):7882.
71. Maluchenko NV, Andreeva TV, Geraskina OV, Gerasimova NS, Lubitelev AV, Feofanov AV, et al. On the Interaction of Resveratrol with Nucleosomes. Biophysics. 2023 Jun;68(3):369–75.
72. Song X, Lei S, Liu S, Liu Y, Fu P, Zeng Z, et al. Catalytically inactive long prokaryotic Argonaute systems employ distinct effectors to confer immunity via abortive infection. Nat Commun. 2023 Nov 1;14(1):6970.
73. Taylor K, Piasecka A, Kajdasz A, Brzęk A, Polay Espinoza M, Bourgeois CF, et al. Modulatory role of RNA helicases in MBNL-dependent alternative splicing regulation. Cell Mol Life Sci. 2023 Nov;80(11):335.
74. Janzen E, Shen Y, Vázquez-Salazar A, Liu Z, Blanco C, Kenchel J, et al. Emergent properties as by-products of prebiotic evolution of aminoacylation ribozymes. Nat Commun. 2022 Jun 25;13(1):3631.
75. Luo SC, Yeh MC, Lien YH, Yeh HY, Siao HL, Tu IP, et al. A RAD51–ADP double filament structure unveils the mechanism of filament dynamics in homologous recombination. Nat Commun. 2023 Aug 17;14(1):4993.

76. Yan J, Liu F, Guan Z, Yan X, Jin X, Wang Q, et al. Structural insights into DNA N6-adenine methylation by the MTA1 complex. Cell Discov. 2023 Jan 20;9(1):8.
77. Weaver TM, Hoitsma NM, Spencer JJ, Gakhar L, Schnicker NJ, Freudenthal BD. Structural basis for APE1 processing DNA damage in the nucleosome. Nat Commun. 2022 Sep 14;13(1):5390.
78. Sheikh AH, Zacharia I, Pardal AJ, Dominguez-Ferreras A, Sueldo DJ, Kim JG, et al. Dynamic changes of the Prf/Pto tomato resistance complex following effector recognition. Nat Commun. 2023 May 4;14(1):2568.
79. Vogel K, Bläske T, Nagel MK, Globisch C, Maguire S, Mattes L, et al. Lipid-mediated activation of plasma membrane-localized deubiquitylating enzymes modulate endosomal trafficking. Nat Commun. 2022 Nov 12;13(1):6897v.
80. Hertz EPT, Vega IA de, Kruse T, Wang Y, Hendriks IA, Bizard AH, et al. The SUMO–NIP45 pathway processes toxic DNA catenanes to prevent mitotic failure. Nat Struct Mol Biol. 2023 Sep;30(9):1303–13.
81. Spinck M, Piedrafita C, Robertson WE, Elliott TS, Cervettini D, De La Torre D, et al. Genetically programmed cell-based synthesis of non-natural peptide and depsipeptide macrocycles. Nat Chem. 2023 Jan;15(1):61–9.
82. Xue L, Schnacke P, Frei MS, Koch B, Hiblot J, Wombacher R, et al. Probing coenzyme A homeostasis with semisynthetic biosensors. Nat Chem Biol. 2023 Mar;19(3):346–55.
83. Wang C, Hesketh EL, Shamorkina TM, Li W, Franken PJ, Drabek D, et al. Antigenic structure of the human coronavirus OC43 spike reveals exposed and occluded neutralizing epitopes. Nat Commun. 2022 May 25;13(1):2921.
84. Seidel M, Becker A, Pereira F, Landry JJM, De Azevedo NTD, Fusco CM, et al. Co-translational assembly orchestrates competing biogenesis pathways. Nat Commun. 2022 Mar 9;13(1):1224.
85. Velusamy A, Sharma R, Rashid SA, Ogasawara H, Salaita K. DNA mechanocapsules for programmable piconewton responsive drug delivery. Nat Commun. 2024 Jan 24;15(1):704.
86. Wang YL, Zhao WW, Bai SM, Feng LL, Bie SY, Gong L, et al. MRNIP condensates promote DNA double-strand break sensing and end resection. Nat Commun. 2022 May 12;13(1):2638.
87. Borges G, Benslimane Y, Harrington L. A CRISPR base editing approach for the functional assessment of telomere biology disorder-related genes in human health and aging. Biogerontology. 2024 Apr;25(2):361–78.
88. Lochs SJA, Van Der Weide RH, De Luca KL, Korthout T, Van Beek RE, Kimura H, et al. Combinatorial single-cell profiling of major chromatin types with MAbID. Nat Methods. 2024 Jan;21(1):72–82.
89. Tang Q, Gulkis M, McKenna R, Çağlayan M. Structures of LIG1 that engage with mutagenic mismatches inserted by polβ in base excision repair. Nat Commun. 2022 Jul 5;13(1):3860.
90. Yang PC, Mahmood T. Western blot: Technique, theory, and trouble shooting. North Am J Med Sci. 2012;4(9):429.
91. Creating relevant cell models. [cited 2024 Apr 10]; Available from: https://www.nature.com/articles/d42473-019-00248-8
92. He SL, Green R. Northern Blotting. In: Methods in Enzymology [Internet]. Elsevier; 2013 [cited 2024 Apr 10]. p. 75–87. Available from: https://linkinghub.elsevier.com/retrieve/pii/B9780124200371000038
93. The challenge – Global Food Security [Internet]. [cited 2024 Apr 11]. Available from: https://www.foodsecurity.ac.uk/challenge/
94. Pixley KV, Falck-Zepeda JB, Paarlberg RL, Phillips PWB, Slamet-Loedin IH, Dhugga KS, et al. Genome-edited crops for improved food security of smallholder farmers. Nat Genet. 2022 Apr;54(4):364–7v.
95. Hoyeraal-Hreidarsson syndrome | Immune Deficiency Foundation [Internet]. [cited 2024 Apr 10]. Available from: https://primaryimmune.org/understanding-primary-immunodeficiency/types-of-pi/hoyeraal-hreidarsson-syndrome
96. Brown T. Southern Blotting. Curr Protoc Immunol [Internet]. 1993 Jun [cited 2024 Apr 10];6(1). Available from: https://currentprotocols.onlinelibrary.wiley.com/doi/10.1002/0471142735.im1006as06
97. Southern Blot [Internet]. [cited 2024 Apr 10]. Available from: https://www.genome.gov/genetics-glossary/Southern-Blot
98. Ran FA, Hsu PD, Wright J, Agarwala V, Scott DA, Zhang F. Genome engineering using the CRISPR-Cas9 system. Nat Protoc. 2013 Nov;8(11):2281–308.
99. Santiago M, Strobel S. Thin Layer Chromatography. In: Methods in Enzymology [Internet]. Elsevier; 2013 [cited 2024 Apr 10]. p. 303–24. Available from: https://linkinghub.elsevier.com/retrieve/pii/B9780124200678000246
100. UNEP [Internet]. 2023 [cited 2024 Apr 10]. What is fuelling the world's antimicrobial resistance crisis? Available from: http://www.unep.org/news-and-stories/story/what-fuelling-worlds-antimicrobial-resistance-crisis
101. Cytiva [Internet]. [cited 2024 Apr 10]. Why choose phosphor imaging for Western blots? Available from: https://www.cytivalifesciences.com/en/us/news-center/phosphorimaging-of-western-blots-10001
102. Hellman LM, Fried MG. Electrophoretic mobility shift assay (EMSA) for detecting protein–nucleic acid interactions. Nat Protoc. 2007 Aug;2(8):1849–61.

103. Selim S. Mechanisms of gram-positive vancomycin resistance (Review). Biomed Rep. 2021 Nov 26;16(1):7.
104. Solon EG, Kraus L. Quantitative whole-body autoradiography in the pharmaceutical industry. J Pharmacol Toxicol Methods. 2001 Sep;46(2):73–81.
105. Brunelle JL, Green R. Coomassie Blue Staining. In: Methods in Enzymology [Internet]. Elsevier; 2014 [cited 2024 Apr 10]. p. 161–7. Available from: https://linkinghub.elsevier.com/retrieve/pii/B9780124201194000136
106. Chevallet M, Luche S, Rabilloud T. Silver staining of proteins in polyacrylamide gels. Nat Protoc. 2006 Nov;1(4):1852–8.
107. Guillen D, Schievelbein M, Patel K, Jose D, Ouellet J. A simple and affordable kinetic assay of nucleic acids with SYBR Gold gel staining. Deng R, editor. PLOS ONE. 2020 Mar 3;15(3):e0229527.
108. https://pubmed.ncbi.nlm.nih.gov/34270053/
109. Magdeldin S, Enany S, Yoshida Y, Xu B, Zhang Y, Zureena Z, et al. Basics and recent advances of two dimensional-polyacrylamide gel electrophoresis. Clin Proteomics. 2014 Dec;11(1):16.

cytiva

cytiva.com

For local office contact information, visit cytiva.com/contact

CY44406-12Jul2024-WH